

Insights into the dynamics of mantle plumes from uranium-series geochemistry

Bernard Bourdon¹†, Neil M. Ribe², Andreas Stracke³†, Alberto E. Saal⁴ & Simon P. Turner⁵

The long-standing paradigm that hotspot volcanoes such as Hawaii or Iceland represent the surface expression of mantle plumes—hot, buoyant upwelling regions beneath the Earth's lithosphere—has recently been the focus of controversy. Whether mantle plumes exist or not is pivotal for our understanding of the thermal, dynamic and compositional evolution of the Earth's mantle. Here we show that uranium-series disequilibria measured in hotspot lavas indicate that hotspots are indeed associated with hot and buoyant upwellings and that weaker (low buoyancy flux) hotspots such as Iceland and the Azores are characterized by lower excess temperatures than stronger hotspots such as Hawaii. This direct link between buoyancy flux and mantle temperature is evidence for the existence of mantle plumes.

The existence of mantle plumes has recently been questioned on the basis of geophysical, petrological and geochemical arguments^{1,2}. Following McKenzie³, we use the term 'plume' in a strictly fluid-dynamical sense, that is "a buoyant upwelling or downwelling whose buoyancy results from the material in the plume being hotter or colder than the surrounding mantle with no implications whatsoever about the depth to which the circulation extends, or about whether or not relative motion between different plumes occurs, or whether the thermal buoyancy is associated with compositional or isotopic variations". According to this definition, evidence for the existence of mantle plumes should come mainly from fluid-dynamical arguments. The persistent difficulty of demonstrating that hotspots are the surface expressions of mantle plumes is due to a number of factors: the poor resolution of geophysical methods, the inability of geophysical and petrological data to show unambiguously that the mantle beneath hot spots is anomalously hot, and the absence of direct geophysical constraints on the velocity of the upwelling mantle.

Recently, however, it has been shown that U-series disequilibria in young hotspot lavas^{4–8} provide a relative measure of mantle upwelling velocity beneath ocean islands. Thus, geochemical data provide important complementary information that is not available from geophysical and petrological data alone. Admittedly, constraining mantle upwelling velocities with U-series data requires that the influence of inter-hotspot differences in the major-element composition of the mantle source during melt production can either be corrected for^{9–11} or is relatively minor. While the role of source heterogeneity on U-series has sometimes been clearly identified (for example, the Sao Miguel island in the Azores region⁶), Stracke *et al.*¹² argue that the role of source heterogeneity on trace-element partitioning during melting beneath ocean islands is subordinate relative to other effects such as variation in mantle upwelling velocity. However, these authors¹² also show that the large variability in mineral/melt partition coefficients for U-series nuclides precludes any definite conclusion on the effect of source heterogeneity⁶ on partitioning behaviour. Accordingly, in the models presented below we assume that the effects of source heterogeneity can be neglected relative to the effects of other key parameters. Our results demonstrate that U-series

data in ocean island lavas provide constraints on mantle upwelling velocity, mantle temperatures (which control the degree of melting) and the horizontal length scale of mantle upwelling, thereby establishing U-series data as a unique link between geochemical and geophysical constraints on mantle dynamics.

U-series systematics in ocean island basalts

The database we have assembled includes new U–Th–Pa mass spectrometry data from the Azores^{6,13,14}, Pitcairn (B.B. *et al.*, manuscript in preparation), the Galapagos islands (A.E.S. *et al.*, manuscript in preparation), and Iceland^{11,12} in addition to published data from Hawaii^{8,15}, the Canary islands¹⁶, the Afar region¹⁷ and Iceland⁷. Other data are from a compilation by Chabaux and Allègre¹⁸. All the samples we consider are lavas from either historical or dated eruptions, so that the effect of radioactive decay since eruption can be either neglected or corrected for. The measurements upon which our analysis is based are the 'activity' ratios (²³⁰Th/²³⁸U) and (²³¹Pa/²³⁵U), where the 'activity' of each nuclide (²³⁰Th, ²³⁸U, ²³¹Pa, or ²³⁵U) is the product λN of its radioactive decay constant λ and its population (number of atoms) N in the sample. As a consequence of the exponential law for radioactive decay, the activity ratio for any two nuclides in a given series is equal to unity if the system is in 'secular equilibrium' (that is, there is a constant population of each nuclide), as is the case in the mantle source before melting. Activity ratios (²³⁰Th/²³⁸U) and (²³¹Pa/²³⁵U) in basalts that differ from unity therefore provide a direct measure of melting-induced fractionation between U–Th and U–Pa, respectively.

On a global scale, there are some remarkable correlations between the U-series data in hotspot lavas and two important geophysical parameters: the buoyancy flux B of the hotspot (essentially the product of the speed, the cross-sectional area, and the density anomaly of the upwelling) and the distance r from the sample to the centre of the hotspot. First, there is a negative correlation between excess ²³⁰Th in the lavas and B (Fig. 1a), first noted by Chabaux and Allègre¹⁸, who proposed that it reflects variations in the degree of melting (see discussion below). Our new data reveal that there is a similar inverse correlation between ²³¹Pa excess and B (Fig. 1b).

¹Laboratoire de Géochimie et Cosmochimie, Institut de Physique du Globe de Paris-CNRS, 4 Place Jussieu, 75252 Paris cedex 05, France. ²Laboratoire de Dynamique des Systèmes Géologiques, Institut de Physique du Globe de Paris-CNRS, 4 Place Jussieu, 75252 Paris cedex 05, France. ³Max-Planck-Institut für Chemie, Abteilung Geochemie, Postfach 3060, 55020 Mainz Germany. ⁴Department of Geological Sciences, Brown University, Providence, Rhode Island 02912, USA. ⁵GEMOC, Department of Earth and Planetary Sciences, Macquarie University, Sydney, New South Wales 2109, Australia. †Present addresses: Institute of Isotope Geochemistry and Mineral Resources, Department of Earth Sciences, ETH Zürich, CH-8092 Zürich, Switzerland.

Second, parent–daughter activity ratios (for example, $^{231}\text{Pa}/^{235}\text{U}$, $^{230}\text{Th}/^{238}\text{U}$) show a positive trend with r for several hotspots, including Hawaii⁸, Iceland⁷ and $^{231}\text{Pa}/^{235}\text{U}$ in the Azores⁶ (Fig. 2) and the Galapagos (A.E.S. *et al.*, manuscript in preparation). In these diagrams, the centre of the hotspot is estimated from geophysical data for Iceland¹⁹ and Hawaii²⁰ and from He isotope data²¹ for the Azores (Fig. 2a). (By contrast, there is no clear trend for the Canaries, where plume–lithosphere interaction may affect the U-series systematics¹⁶). The correlations shown in Figs 1 and 2 are intriguing because they directly relate the geochemical characteristics of erupted lavas to geophysical parameters of the underlying mantle (for example, mantle temperature, upwelling velocity, and possibly the degree of melting¹⁸). We now propose a model to quantify the influence of these parameters on the U-series systematics of erupted lavas.

Inferences of temperature and upwelling velocity beneath hotspots

To model theoretically the relationship between U-series disequilibrium and buoyancy flux (Fig. 1), we make two reasonable simplifying assumptions. First, we suppose that the melt productivity (percent-

age melt per kbar) is constant, which implies that the mantle upwelling velocity is linearly related to the melting rate (in kg of melt per cubic metre per year). Second, we assume that there exists a simple quantitative relationship between B and the mantle upwelling velocity W (for example, $B \propto W^2$; ref. 4). In this case, melting models^{5,18,22} that include the melting rate and assume that melt is extracted from the matrix once a critical porosity is reached predict that activity ratios (such as $^{231}\text{Pa}/^{235}\text{U}$ or $^{230}\text{Th}/^{238}\text{U}$) in the melt should be inversely related to the upwelling velocity (Fig. 3). On this basis, we used the dynamic melting equation given in ref. 22 to calculate the activity ratios ($^{231}\text{Pa}/^{235}\text{U}$) or ($^{230}\text{Th}/^{238}\text{U}$) in the melt as a function of buoyancy flux, assuming that the melting rate, excess temperature, viscosity and total extent of melting are all constant. This model predicts that ($^{231}\text{Pa}/^{235}\text{U}$) in the melt decreases as B increases, reaching a value of unity for very large B . This first-order approach supports the idea that variations in the magnitude of U-series disequilibrium are mainly controlled by variations in mantle upwelling rates. This differs from the conclusion of ref. 18 that the controlling factor is the degree of melting F_{max} . However, variations in F_{max} , while they may cause some dispersion in the observed relationships, cannot explain the overall trend shown on Fig. 1, because the Hawaii, Iceland and Afar samples include both high-degree and low-degree melts (tholeiites and alkali basalts, respectively) while the Canaries, Azores, Samoa and Pitcairn samples are exclusively low-degree melts (alkali basalts).

Although the simple melting model used above lends plausibility to the hypothesis that U-series systematics are controlled by the upwelling velocity, it neglects important thermal aspects of the problem such as differences of mantle temperature beneath different hotspots, the temperature-dependence of mantle viscosity, and the fact that weaker plumes (those with lower B) cool more than stronger plumes as they ascend²³. Accordingly, we now test the robustness of our preliminary conclusion using a more sophisticated plume model²⁴ that properly incorporates thermal effects. According to this model, the excess temperature ΔT_{top} , at the top of a plume (that is, just beneath the lithosphere) can be calculated as a function of the excess temperature ΔT_{bottom} at the plume's depth of origin by:

$$\Delta T_{\text{top}} = \Delta T_{\text{bottom}} \exp \left[- \frac{4\pi k\alpha}{\beta C_p B} z \right] \quad (1)$$

where B is the buoyancy flux, β is a parameter describing the dependence of viscosity on temperature, and the remaining parameters are defined in Supplementary Table 1. Although equation (1) neglects the dependence of thermal conductivity (k) and thermal expansivity (α) on pressure, its predictions are similar to those of more realistic models²³, and it can therefore be used to calculate the relationships among B , ΔT_{top} and ΔT_{bottom} (Supplementary Fig. 1). For a given buoyancy flux B , ΔT_{top} depends strongly on ΔT_{bottom} , except for low buoyancy fluxes where ΔT_{top} is relatively low and less dependent on the initial ΔT_{bottom} . According to ref. 25, mantle plumes may be of different types with different values of ΔT_{bottom} , depending on the depth where the plume originates and on the volume of the hot boundary layer that it samples. In applying equation (1), therefore, we treated ΔT_{bottom} and B as variable input parameters and then calculated the U-series signature in the erupted melt using a dynamic melting model (see Supplementary information). The model accounts for the fact that upwelling material that is hotter begins to melt at a greater depth, and also (by extension) for the fact that the degree of melting is larger for greater initial depths of melting.

The results of the calculations (Fig. 4) show that the observations are well explained by moderate (50–200 °C) values of the top excess temperature ΔT_{top} . According to Supplementary Fig. 1, these values of ΔT_{top} correspond to values of ΔT_{bottom} that are much smaller than the temperature jump across the boundary layer at the core–mantle boundary, which may be as much as 1,300 °C (ref. 26). This would indicate that only the upper part of the thermal boundary layer is

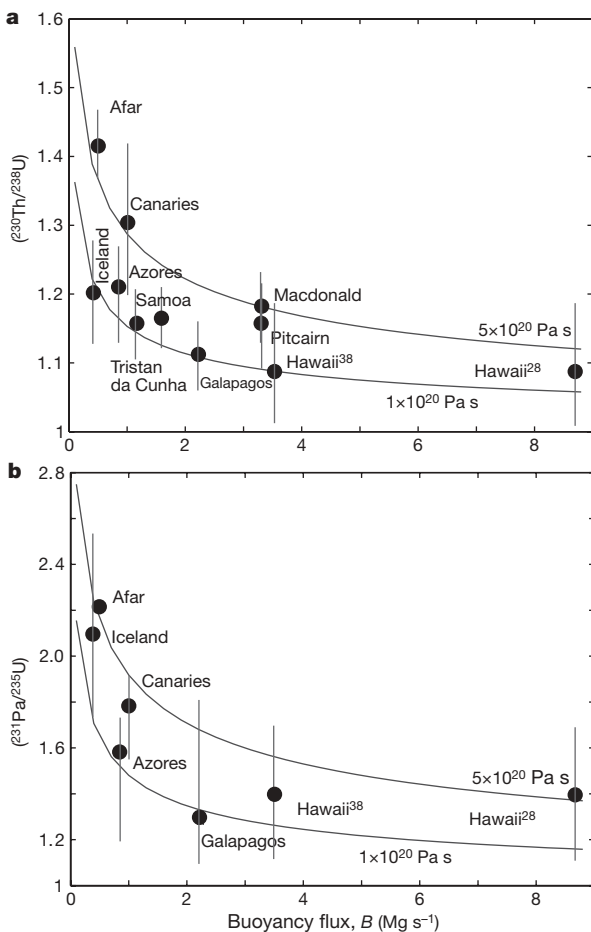


Figure 1 | U-series activity ratios versus buoyancy fluxes for recent hotspot lavas. $^{230}\text{Th}/^{238}\text{U}$ (a) and $^{231}\text{Pa}/^{235}\text{U}$ (b) activity ratios versus buoyancy fluxes for recent hotspot lavas. The mean for each hotspot is shown by a black circle and the range by a vertical line. Both diagrams show a negative trend, despite relatively large uncertainties in the estimation of buoyancy fluxes. This trend can be explained by variation in upwelling velocities. Other possibilities are discussed in detail in the text. Buoyancy fluxes are taken from ref. 38 when available, except for Hawaii where the estimates of both ref. 38 and ref. 28 are given. Curves in a and b are labelled with viscosity at the axis of the plume. The model curves were calculated with a dynamic melting model with constant melt productivity, constant viscosity and excess temperature (see Supplementary information for description of the model).

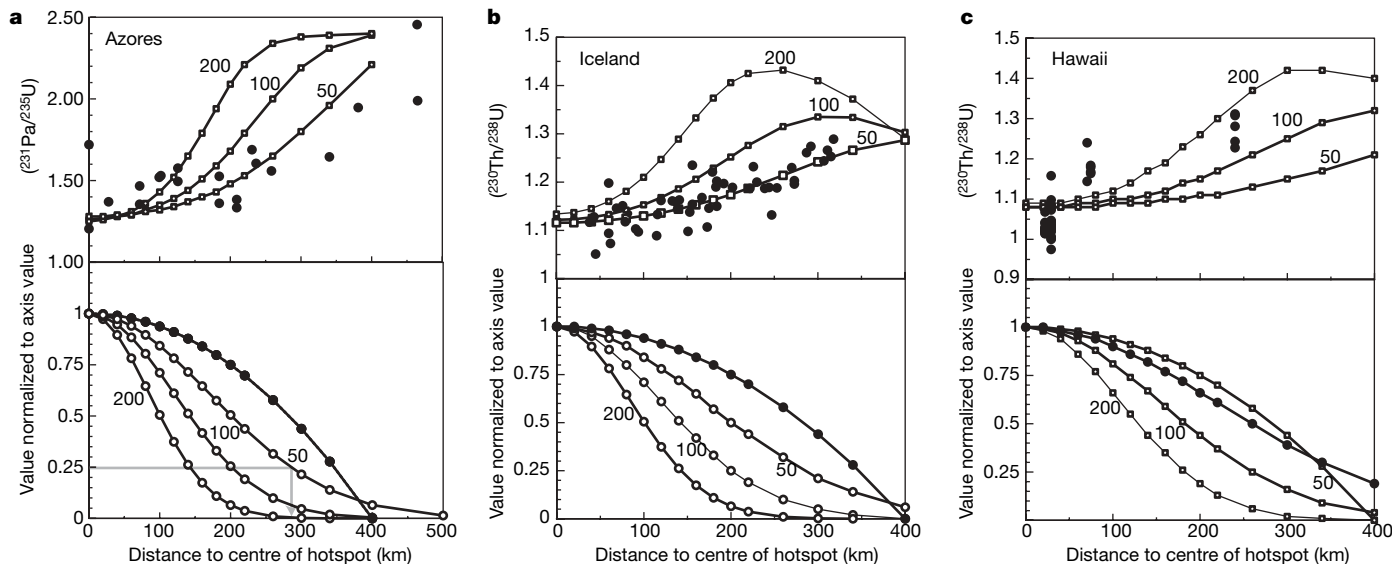


Figure 2 | U-series activity ratios as a function of distance from the centre of hotspots. **a**, $(^{231}\text{Pa}/^{235}\text{U})$ activity ratios plotted as a function of the distance from the centre of the Azores hotspot (data from ref. 6). **b**, $(^{230}\text{Th}/^{238}\text{U})$ activity ratios plotted as a function of the distance from the centre of the Iceland hotspot (data from ref. 7). **c**, $(^{230}\text{Th}/^{238}\text{U})$ activity ratios plotted as a function of the distance from the centre of the Hawaii hotspot (data as in ref. 5). The curves are calculated using a dynamic melting model and an analytical model for an axisymmetric plume²⁴. The bottom panels show the profiles of excess temperature (black symbols) and upwelling velocity (white symbols) predicted by the model, normalized to their

maximum values at the plume axis. The excess temperature at the top of the plume relative to the ambient mantle (numbers on curves) was adjusted to give the best fit to the observations. The best fit to the Hawaii data was estimated to be 200 °C based on the combined ^{230}Th and ^{231}Pa data set (not shown). The degree of melting used in the model is a function of the initial melting temperature. The melts are assumed to move vertically with no lateral mixing. The radius of the plume (r_{25}) is defined by the distance from the centre of the plume where $W = 0.25W_0$, where W_0 is the axial upwelling velocity.

being sampled by those plumes that originate from the core–mantle boundary²⁷.

The calculations also show that the dependence of $(^{231}\text{Pa}/^{235}\text{U})$ and $(^{230}\text{Th}/^{238}\text{U})$ on ΔT_{bottom} is weak and has little influence on the model curves on Fig. 4. These curves further show that the observations can be explained by initial excess temperatures ΔT_{bottom} in the range 100–300 °C, which is consistent with geophysical inferences²⁸ and geochemistry²⁹. Because plumes with low buoyancy fluxes cool more during upwelling, ΔT_{top} is an increasing function of B (50–70 °C for the Azores, more than 100 °C for Iceland, 200 °C for Hawaii; see below and also Supplementary Fig. 1). The estimate for Iceland is in good agreement with one obtained by comparing the observed topography along the Reykjanes ridge with that predicted by a three-dimensional convection model³⁰. The larger estimate

($\Delta T_{\text{top}} \approx 180$ °C) determined by ref. 31 using a different three-dimensional convection model relies on the amount of water present in the Icelandic mantle source, a parameter that is not well constrained.

Several studies have shown that the melting process can be strongly influenced by the presence of water in the mantle source of hot spot lavas^{7,31,32}. To take this added complexity into account, we have included the effect of water in the model (see Supplementary Information) by decreasing the initial melting rate and increasing the initial temperature of melting. Although these effects shift the model curves slightly (by at most 10–15%), the overall shape of the curves and the ranges in $(^{230}\text{Th}/^{238}\text{U})$ and $(^{231}\text{Pa}/^{235}\text{U})$ are not much affected.

The presence of water can also affect the mechanical properties of the source region where melting occurs. In particular, melting results in rapid dehydration of the source material, which can increase its viscosity by a factor of seven and thereby reduce its upwelling velocity^{7,31}. Yet, as shown by Asimow *et al.*³³, the concurrent increase in melt productivity (by a factor of 30) largely compensates for the changes due to viscosity. Taken together, the above points confirm that the observed trends of U-series activity ratios as a function of buoyancy flux (Fig. 2a and b) are mainly due to variations in upwelling velocity.

An important consequence of our modelling is that the mantle upwelling velocities can be estimated and compared with the surface plate speeds, which in turn should be comparable to upper mantle convection velocities. For plumes with low buoyancy flux (0.5 – 2 Mg s^{-1}) the calculated upwelling velocities range from 2 to 6 cm yr^{-1} , which is similar to spreading rates at mid-ocean ridges.

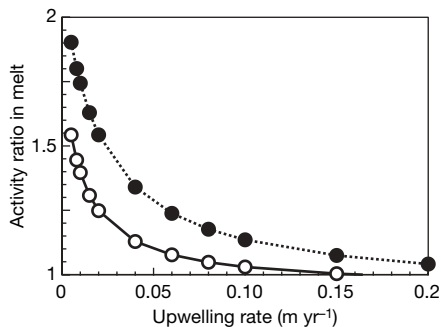


Figure 3 | Relationship between U-series activity ratios in erupted melts and mantle upwelling velocity. Open circles represent $(^{230}\text{Th}/^{238}\text{U})$ and solid circles represent $(^{231}\text{Pa}/^{235}\text{U})$. Model curves were calculated using the dynamic melting model of ref. 18 assuming constant melt productivity (that is, a linear dependence of the degree of melting on the upwelling velocity). $(^{231}\text{Pa}/^{235}\text{U})$ activity ratios are more sensitive to mantle upwelling velocity than $(^{230}\text{Th}/^{238}\text{U})$ activity ratios. The model assumes partition coefficients $D^{\text{U}} = 3.4 \times 10^{-3}$, $D^{\text{Th}} = 1.2 \times 10^{-3}$, $D^{\text{Pa}} = 7 \times 10^{-5}$, a porosity $\phi = 3 \times 10^{-3}$, and a maximum degree of melting $F_{\text{max}} = 0.05$.

The width of mantle plumes

Because the analytical model of Olson *et al.*²⁴ predicts radial profiles of the vertical velocity and the excess temperature across an upwelling plume, it can be used in conjunction with the trends shown on Fig. 2 to estimate the radii of the Iceland, Azores and Hawaii plumes at the depth where melting occurs. The calculation comprises two steps.

First, we have used the analytical solution for axisymmetric mantle plumes derived by Olson *et al.*²⁴ to infer the temperature and vertical velocity field using the buoyancy flux and excess temperature as input parameters (see Supplementary information). Second, these parameters were used to calculate ^{230}Th - and ^{231}Pa -excess in the melt using a dynamic melting model¹⁸. The excess temperature ΔT_{top} was then adjusted to match the observed increase of ^{230}Th - and ^{231}Pa -excess as a function of distance to the centre of the hotspot (Fig. 2).

For the sake of comparison, we define the radius of the plume as the radius ($= r_{25}$) for which the upwelling velocity is 25% of its value on the plume axis. On the basis of Fig. 2, $r_{25} = 220 \pm 40$ km, 280 ± 40 km and 290 ± 50 km for Hawaii, Iceland and the Azores, respectively (see Fig. 2 legend). The radius determined for Iceland compares well with the estimate of ref. 30, based on a three-dimensional convection model. Because these radii are values at the depth of melting (60–100 km), they cannot be compared directly with the width of a plume conduit, because a plume impinging on the base of

the lithosphere broadens as it decelerates. Nevertheless, our estimates are not inconsistent with estimates from seismology^{34,35} based on inversion of body waves (at a depth of 300 km). Because the viscosity of mantle materials depends strongly on temperature, the radius of the thermal halo is significantly greater than r_{25} (the radius of the region of fast upwelling). If the mantle surrounding the plume conduit melts owing to conductive heating (for example, along a mid-ocean ridge in the case of near-ridge hotspots) and the melts rise vertically, our model predicts that the radius of the compositional and bathymetry anomalies observed around hotspots should be broader than the upwelling velocity profile depicted in Fig. 2.

In the case of the Azores, there is fairly clear evidence that the geochemical anomaly is broader than the inferred zone of extensive upwelling (see Fig. 5 and ref. 36), despite the paucity of U-series data for distances greater than about 300 km away from the plume centre. For Iceland, there is a limited data set for the Reykjanes ridge^{36,37}, which also suggests that the radiogenic isotope anomalies (Sr, Nd, Pb) extend beyond approximately 500 km, whereas the U-series signal probably tapers off at about 300–400 km away from the plume centre^{7,36}. While a more detailed examination of this issue awaits more comprehensive data sets, the available data are at least consistent with the model prediction.

The correlations between U-series disequilibria in ocean island lavas and buoyancy fluxes can be explained by coupled variations in mantle temperature and upwelling velocities. Our modelling provides evidence that hotspots are associated with increased buoyancy and temperature of the upwelling mantle: that is, they correspond to mantle plumes as defined above. The mantle upwelling velocities associated with low-buoyancy-flux hotspots are comparable to surface plate speeds, which implies that plumes are likely to be affected by upper mantle convection. It is thus possible that the position of low-buoyancy-flux plumes is not fixed.

In addition, our modelling provides constraints on the lateral extent of mantle upwelling for the Azores (220 ± 40 km), Hawaii (280 ± 40 km) and Iceland (290 ± 50 km). These are greater than some earlier estimates but comparable to estimates from seismology. The predicted temperature excesses at the top of the upwelling mantle column are 200°C (Hawaii), $70\text{--}80^\circ\text{C}$ (Iceland) and 50°C (Azores), respectively. At least in the case of the Azores and Iceland, the thermal halo surrounding the mantle plumes is wider than the region of intense upwelling. Unfortunately, our model calculations are not highly sensitive to the excess temperature in the boundary layer from which the upwelling mantle originates, making it difficult to determine the depth of this layer in the mantle.

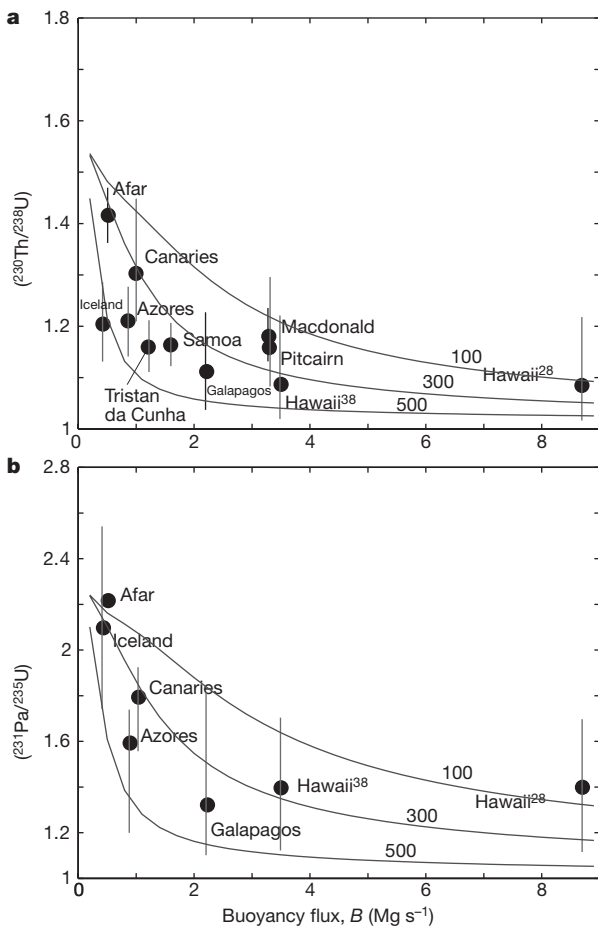


Figure 4 | Models of U-series activity ratios versus buoyancy flux for recent hotspot lavas. a, ($^{230}\text{Th}/^{238}\text{U}$). b, ($^{231}\text{Pa}/^{235}\text{U}$). U-series data sources are given in the section ‘Inferences of temperature and upwelling velocity beneath hotspots’. The plotted data represent an average of published data (data source as in Fig. 2). The vertical bars represent the dispersion of the data, that is, a 1σ standard deviation calculated based on all existing data. See caption of Fig. 1 for source of buoyancy fluxes. The model curves are labelled with the excess temperature in the boundary layer generating the plume (100, 300 and 500°C). The melting rate Γ in percentage of melt per kbar is assumed to depend on pressure³² as $\Gamma = \Gamma_0 e^{-\beta(P - P_0)}$, where β is an adjustable parameter (see also ref. 6) and P is the pressure in kbar. We assume that $\Gamma = 3$ and 0.15% kbar $^{-1}$ at $P = 7$ and 30 kbar, respectively, similar to the values in ref. 6. Partition coefficients for U, Th and Pa are as in ref. 6.

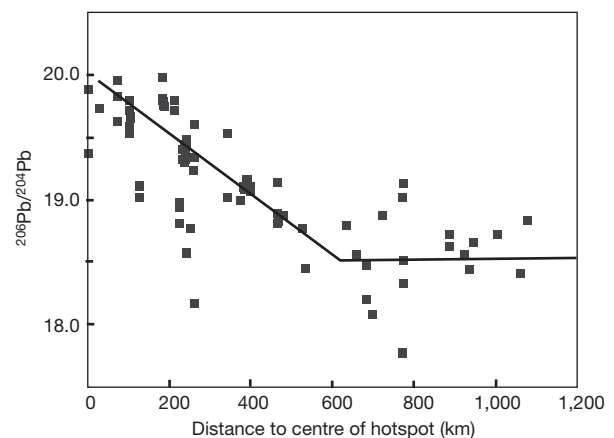


Figure 5 | $^{206}\text{Pb}/^{204}\text{Pb}$ as a function of the distance from the centre of the Azores hotspot. Although there is considerable spread in this data set, there is a marked decrease of $^{206}\text{Pb}/^{204}\text{Pb}$ for distances up to 600 km, beyond which the variation is limited. For data sources, see text.

Received 18 May; accepted 9 October 2006.

1. Foulger, G. R. *et al.* Seismic tomography shows that upwelling beneath Iceland is confined to the upper mantle. *Geophys. J. Int.* **146**, 504–530 (2001).
2. Meibom, A. *et al.* Are high $^3\text{He}/^4\text{He}$ ratios in oceanic basalts an indicator of deep-mantle plume components? *Earth Planet. Sci. Lett.* **208**, 197–204 (2003).
3. McKenzie, D. *et al.* Source enrichment processes responsible for isotopic anomalies in oceanic island basalts. *Geochim. Cosmochim. Acta* **68**, 2699–2724 (2004).
4. Bourdon, B., Joron, J. L., Claude-Ivanaj, C. & Allegre, C. J. U-Th-Pa-Ra systematics for the Grande Comore volcanics: melting processes in an upwelling plume. *Earth Planet. Sci. Lett.* **164**, 119–133 (1998).
5. Bourdon, B. & Sims, K. W. W. in *U-series Geochemistry* (eds Bourdon, B., Lundstrom, C., Henderson, G. & Turner, S. P.) 215–253 (Mineralogical Society of America, 2003).
6. Bourdon, B., Turner, S. P. & Ribe, N. M. Partial melting and upwelling rates beneath the Azores from a U-series isotope perspective. *Earth Planet. Sci. Lett.* **239**, 42–56 (2005).
7. Kokfelt, T. F., Hoernle, K. & Hauff, F. Upwelling and melting of the Iceland plume from radial variation of ^{238}U - ^{230}Th disequilibria in postglacial volcanic rocks. *Earth Planet. Sci. Lett.* **214**, 167–186 (2003).
8. Sims, K. W. W. *et al.* Porosity of the melting zone and variations in the solid mantle upwelling rates beneath Hawaii: Inferences from ^{238}U - ^{230}Th - ^{226}Ra , and ^{235}U - ^{231}Pa disequilibria. *Geochim. Cosmochim. Acta* **63**, 4119–4138 (1999).
9. Sigmarsson, O., Carn, S. & Carracedo, J. Systematics of U-series nuclides in primitive lavas from the 1730–36 eruption on Lanzarote, Canary islands, implications for the role of garnet-pyroxenite during oceanic basalt formations. *Earth Planet. Sci. Lett.* **162**, 137–151 (1998).
10. Stracke, A., Salters, V. J. M. & Sims, K. W. W. Assessing the presence of garnet-pyroxenite in the mantle sources of basalts through combined hafnium-neodymium-thorium isotope systematics. *Geochem. Geophys. Geosyst.* **1**, doi:10.1029/1999GC000013 (1999).
11. Stracke, A. *et al.* The dynamics of melting beneath Theistareykir, northern Iceland. *Geochem. Geophys. Geosyst.* **4**, 8513, doi:10.1029/2002GC000347 (2003).
12. Stracke, A., Bourdon, B. & McKenzie, D. Melt extraction in the Earth's mantle: Constraints from U-Th-Pa-Ra studies in oceanic basalts. *Earth Planet. Sci. Lett.* **244**, 97–112 (2006).
13. Bourdon, B., Langmuir, C. H. & Zindler, A. Ridge-hotspot interaction along the Mid-Atlantic Ridge between $37^{\circ}30'$ and $40^{\circ}30'\text{N}$: The U-Th disequilibrium evidence. *Earth Planet. Sci. Lett.* **142**, 175–189 (1996).
14. Turner, S., Hawkesworth, C., Rogers, N. & King, P. U-Th isotope disequilibria and ocean island basalt generation in the Azores. *Chem. Geol.* **139**, 145–164 (1997).
15. Sims, K. W. W. *et al.* Mechanisms of magma generation beneath Hawaii and midocean ridges—uranium/thorium and samarium/neodymium isotopic evidence. *Science* **267**, 508–512 (1995).
16. Lundstrom, C. C., Hoernle, K. & Gill, J. B. U-series disequilibria in volcanic rocks from the Canary Islands: Plume versus lithospheric melting. *Geochim. Cosmochim. Acta* **67**, 4153–4177 (2003).
17. Vigier, N., Bourdon, B., Joron, J. L. & Allègre, C. J. U-decay series and trace element systematics in the 1978 eruption of Ardoukoba, Asal rift: timescale of magma crystallization. *Earth Planet. Sci. Lett.* **174**, 81–97 (1999).
18. Chabaux, F. & Allègre, C. J. ^{238}U - ^{230}Th - ^{226}Ra disequilibria in volcanics—a new insight into melting conditions. *Earth Planet. Sci. Lett.* **126**, 61–74 (1994).
19. MacLennan, J., McKenzie, D. & Groenvold, K. Plume-driven upwelling under central Iceland. *Earth Planet. Sci. Lett.* **2001**, 67–82 (2002).
20. DePaolo, D. J. & Stolper, E. M. Models of Hawaiian volcano growth and plume structure. Implications of results from the Hawaii Scientific Drilling Project. *J. Geophys. Res.* **101**, 11643–11654 (1996).
21. Moreira, M. *et al.* Helium and lead isotope geochemistry of the Azores Archipelago. *Earth Planet. Sci. Lett.* **169**, 189–205 (1999).
22. Richardson, C. & McKenzie, D. Radioactive disequilibria from 2D models of melt generation by plumes and ridges. *Earth Planet. Sci. Lett.* **128**, 425–437 (1994).
23. Albers, M. & Christensen, U. R. The excess temperature of plumes rising from the core-mantle boundary. *Geophys. Res. Lett.* **23**, 3567–3570 (1996).
24. Olson, P., Schubert, G. & Anderson, C. Structure of axisymmetric plumes. *J. Geophys. Res.* **98**, 6829–6844 (1993).
25. Courtillot, V., Davaille, A., Besse, J. & Stock, J. Three distinct types of hotspots in the Earth's mantle. *Earth Planet. Sci. Lett.* **205**, 295–308 (2003).
26. Boehler, R., Chopelas, A. & Zerr, A. Temperature and chemistry of the core-mantle boundary. *Chem. Geol.* **120**, 199–206 (1995).
27. Farnetani, C. G. Excess temperature of mantle plumes: The role of chemical stratification across D. *Geophys. Res. Lett.* **24**, 1583–1586 (1997).
28. Sleep, N. H. Hotspots and mantle plumes—some phenomenology. *J. Geophys. Res.* **95**, 6715–6736 (1990).
29. Schilling, J.-G. Fluxes and excess temperatures of mantle plumes inferred from their interaction with migrating mid-ocean ridges. *Nature* **352**, 397–403 (1991).
30. Ribe, N. M., Christensen, U. R. & Theissing, J. The dynamics of plume ridge interaction. 1: Ridge centered plumes. *Earth Planet. Sci. Lett.* **134**, 155–168 (1995).
31. Ito, G., Shen, Y., Hirth, G. & Wolfe, C. J. Mantle flow, melting, and dehydration of the Iceland mantle plume. *Earth Planet. Sci. Lett.* **165**, 81–96 (1999).
32. Asimow, P. D., Dixon, J. E. & Langmuir, C. H. A hydrous melting and fractionation model for mid-ocean ridge basalts: Application to the Mid-Atlantic ridge near the Azores. *Geochem. Geophys. Geosyst.* **5**, 24, doi:10.1029/2003GC000568 (2004).
33. Asimow, P. D. & Langmuir, C. H. The importance of water to oceanic mantle melting regimes. *Nature* **421**, 815–820 (2003).
34. Montelli, R. *et al.* Finite-frequency tomography reveals a variety of plumes in the mantle. *Science* **303**, 338–343 (2004).
35. Wolfe, C., Bjarnason, I. T., Van Decar, J. & Solomon, S. C. Seismic structure of the Iceland mantle plume. *Nature* **385**, 245–247 (1997).
36. Murton, B. J., Taylor, R. N. & Thirlwall, M. F. Plume-ridge interaction: a geochemical perspective from the Reykjanes ridge. *J. Petrol.* **43**, 1987–2012 (2002).
37. Peate, D. W. *et al.* ^{238}U - ^{230}Th constraints on mantle upwelling and plume-ridge interaction along the Reykjanes ridge. *Earth Planet. Sci. Lett.* **187**, 259–272 (2001).
38. Ribe, N. M. The dynamics of plume ridge interaction. 2: Off-ridge plumes. *J. Geophys. Res.* **101**, 19195–19204 (1996).

Supplementary Information is linked to the online version of the paper at www.nature.com/nature.

Acknowledgements We thank D. McKenzie for the support of A.S. during his visit to IPGP. A.E.S.'s visit to Paris was supported by IPGP funds. We also thank D. McKenzie, A. Davaille, M. Moreira and C. Farnetani for numerous discussions about plumes. We are grateful to P. Olson and T. Kokfelt for comments.

Author Information Reprints and permissions information is available at www.nature.com/reprints. The authors declare no competing financial interests. Correspondence and requests for materials should be addressed to B.B. (bourdon@erdw.ethz.ch).